Numerical evaluation of multipass welding temperature field in API 5L X80 steel welded joints

J. A. da Nóbrega[1,a], D. D. Diniz Silva [1,b], B. A. Araújo[2,c], R. H. F. de Melo[1,d], T. M. Maciel[1,e], A. A. Silva[1,f], N. C. N. dos Santos[2,g]

[1] Federal University of Campina Grande, Campina Grande-PB, Brazil

[2] Federal Institute of Education and Technology, Paraiba, Brazil

[a]jailson_engmec@hotmail.com, [b]diego_leader@yahoo.com.br, [c]bengmec@yahoo.com.br, [d]raphael.engmec@gmail.com, [e]theo@dem.ufcg.edu.br, [f]almeida@dem.ufcg.edu.br, [g]neilorcesar@gmail.com.

ABSTRACT

Many are the metallurgical changes suffered by materials when subjected to welding thermal cycle, promoting a considerable influence on the welded structures thermo mechanical properties. In project phase, one alternative for evaluating the welding cycle variable, would be the employment of computational methods through simulation. So, this paper presents an evaluation of the temperature field in a multipass welding of API 5L X80 steel used for oil and gas transportation, using the ABAQUS ® software, based on Finite Elements Method (FEM). During the simulation complex phenomena are considerable including: Variation in physical and mechanical properties of materials as a function of temperature, welding speed and the different mechanisms of heat exchange with the environment (convection and radiation) were used. These considerations allow a more robust mathematical modeling for the welding process. An analytical heat source proposed by Goldak, to model the heat input in order to characterize the multipass welding through the GTAW (Gas Tungsten Arc Welding) process on root and the SMAW (Shielded Metal Arc Welding) process for the filling passes were used. So, it was possible to evaluate the effect of each welding pass on the welded joint temperature field, through the temperature peaks and cooling rates values during the welding process.

Keywords: Multipass welding, Temperature field, Weld thermal cycles, Finite element method, Computer simulation

1. INTRODUCTION

Many are the transformations involved in the welding process due to the intense addition of heat which happens to non-uniform and transient manner, particularly in fusion welding, being of fundamental importance to study the evolution of the temperature field in the vicinity of the weld, to minimize thermal effects due to weld parameters as preheating temperature. The variation of preheating temperature, for instance, causes variation in cooling rate, which can causes modifications in phase transformations temperature, changing the welded joint mechanical properties.

The welded joint microstructure is dependent on the base metal chemical composition, grain size and cooling rate. So, the estimation of the welding thermal cycle variable is of fundamental importance in controlling the formation of fragile microstructures susceptible to crack formation [1]. The estimated peak temperature in turn enables the indirect assessment of grain size of austenite which in turn affects the position of the cooling curves of the material and, consequently, the microstructure resulting in welded joint. In order to reduce costs and time experimental methods to obtain the temperature distributions, and computational program to estimate the temperature fields in welded joints using analytical techniques have been developed [2].

The purpose of this study was to simulate and evaluate the temperature field in API 5L X80 steel welded joint by GTAW (Gas Tungsten Arc Welding) and SMAW (Shielded Metal Arc Welding) process using a commercial software based on the Finite Element Method (FEM) enabling the evaluation of variations and the effect of each pass in the process.

2. THERMAL MODELING

In the electric arc welding process, an electrical source generates a power difference U between the electrode and the base metal, inducing the formation of an electric arc traversed by a current. In the process, there are losses by several factors, among them we can mention the convection and radiation in the arc and the electrode. So, only a portion of this energy is used to melt the material, being necessary to add a variable called efficiency of power (η). Therefore the actual weld heat input should be represented by the expression (1):

$$Q = \eta . U . I . \tag{1}$$

For this thermal model the heat flux expression on Eq. (2) which is allowed to assess the thermal gradient in a three-dimensional object via an energy balance on a control volume in the study area was used. According to [3], the heat flow is not linear on the piece because the thermophysical properties of materials are highly dependent on temperature.

$$\rho(T)c(T)\frac{\partial T}{\partial t} = Q + \frac{\partial}{\partial x}\left[K_x(T)\frac{\partial T}{\partial x}\right] + \frac{\partial}{\partial y}\left[K_y(T)\frac{\partial T}{\partial y}\right] + \frac{\partial}{\partial z}\left[K_z(T)\frac{\partial T}{\partial z}\right] \tag{2}$$

In Eq (2) ρ is the density, c is the specific heat and Q is the heat input (Eq. 1). *Kx, Ky, Kz* are the coefficients of thermal conductivity in all three directions, T is temperature and t is time.

The heat loss by convection (q_c) and radiation (q_r) can be measured using the following expressions:

$$q_c = h_f(T - T_\infty) \tag{3}$$

$$q_r = \varepsilon\sigma(T^4 - T_\infty^4) \tag{4}$$

where h_f is the convective coefficient, T_∞ is the ambient temperature, σ is the Stefan-Boltzmann constant and ε is the emissivity of the surface of the body.

The phase change occurring during the process, known as latent heat can be expressed as a function of enthalpy H by the following equation:

$$H = \int \rho c\, dT \tag{5}$$

For analysis by FEM, an essential point in the simulation is the modeling of the heat source. Goldak proposed an analytical solution for modeling which is currently used in this analysis and the distributed heat source associated with arc welding. This became possible the determination of the temperature field computationally. An 3D finite Gaussian on a double ellipsoid, as shown in Fig. (1) was considered. This source is defined analytically by Eqs. (6) and (7) [4].

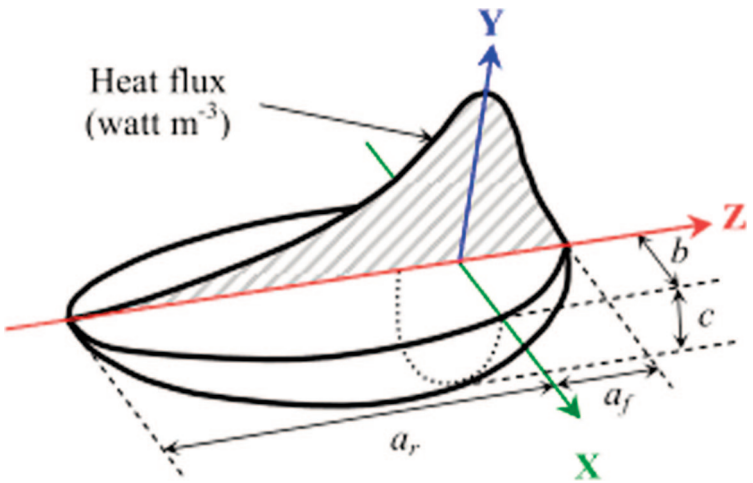

Figure 1: 3D Volumetric Gaussian on a double ellipsoidal of radius a, b and c [4]

$$q_f(x,y,z) = f_f \frac{\eta UI}{a_f bc\pi\sqrt{\pi}} 6\sqrt{3} \exp\left(\frac{-3x^2}{a_f^2}\right) \exp\left(\frac{-3y^2}{b^2}\right) \exp\left(\frac{-3z^2}{c^2}\right) \quad (6)$$

$$q_r(x,y,z) = f_r \frac{\eta UI}{a_r bc\pi\sqrt{\pi}} 6\sqrt{3} \exp\left(\frac{-3x^2}{a_r^2}\right) \exp\left(\frac{-3y^2}{b^2}\right) \exp\left(\frac{-3z^2}{c^2}\right) \quad (7)$$

where q_f and q_r are the volumetric distributions of energy before and after the torch [W.m^{-3}], f_f and f_r are the distributions of energy before and after the torch; a_f and a_r are the lengths of the weld pool before and after the torch [m] b is the half width of the weld pool [m] and c is the depth of the fused zone [m], as shown in Fig (1).

U, I, η parameters are directly linked to welding procedure, while b and c are the geometric parameters of the source and can be determined by metallographic examination. The other parameters a_f, a_r, f_f and f_r are obtained through the parameters b and c, furthermore, the sum of f_f and f_r is equal to 2 [5]. In the absence of better data, the distance from the front of the heat source is the same to half the width of the weld and the distance behind the heat source is equal to twice the width, achieving this way good approximation [4].

Thermal analysis for reliable welding due to the increased requirements and control of modern steels is of great importance correct dimensioning of the preheating temperature of the base material. Based on the standard [6], [7] describes in his dissertation, two formulas for calculating the preheating temperature. The first one is most often employed and uses the value of carbon equivalent (CE) of steel for this purpose. The CE is an expression that considers not only the percentage of carbon as well as the percentage of other elements of the steel alloy that affects their hardenability. There is more than one expression for calculation of CE value. The most commonly used is that proposed by the International Institute of Welding (IIW), valid for steels containing more than 0.12% carbon. The other formula suggests the value of the preheating temperature according to the Pcm (critical metal parameter), which is another based on the chemical composition of the steel parameter. Both expressions (CE and Pcm) were created to assess the susceptibility of the steel to the formation of hydrogen-induced cracking [7].

Four methods for calculating the preheating temperature for structural steels including the API 5L grade X80 are compared by [7]. The four methods are: a) the method of *British Standard Institution,* BS 5135, based on the CE value (IIW), b) the method of American Welding Society (AWS D1.1) which calculates the temperature of preheating means Pcm, c) the method of CET (Total carbon equivalent) which calculates the temperature of preheating as a function of its CE, material thickness, diffusible hydrogen in the weld metal and the welding power, and d) the method of CE_N. It follows that for API 5L X80 steel, the methods AWS and CE_N not require the use of preheating temperature, however, the methods BS and CET were more conservative, when preheating is needed in welding of API 5L X80 steel.

In this work the preheating temperature value was based on the study of [7]. Thus, the room temperature (25°C) was selected considering the CEN methods as recommended by the AWS for this type of steel. The preheating temperature value was 100°C corresponding to the BS method, which is the most conservative from those presented by Cooper [8]. The interpass temperature value was 150°C following the standard [9].

3. MATERIAL AND COMPUTATIONAL METHOD

The computational model was developed with the assistance of the calculation code ABAQUS® 6.9, which is based on the finite element method (FEM). The workpiece was an API 5L X80 steel plate with 0.120 m x 0.360 m x 0.017 m. The API 5L X80 steel chemical composition is shown in Tab (1).

The simulation was performed using three welding conditions and two welding process. The two first condition was using the GTAW process for the root pass (GTAW-R) and the SMAW (SMAW-FP1) for the filling pass without preheating, and with preheating temperature of 100°C, and the third condition, was using the SMAW welding process for the root (SMAW-R) and filler pass (SMAW-FP2) at the same preheating temperature (100°C). Furthermore, an interpass temperature of 150°C was used following the standard [9]. For modeling the heat source a subroutine in Fortran DFLUX environment was used. The principals welding parameters are shown in Tab. (2) according by [10].The value of η for calculating the arc heat input was 65% to GTAW process and 80% for the SMAW process [11]. The computer system was programmed to start a new pass welding, when the interpass temperature value in the plate was reached.

The multipass simulation was developed following the guidelines of a weld made in laboratory. The first pass welding was held in the XY plane, moving the Y axis. The second

Table 1: Chemical composition of API 5L X80 steel

				Percentage (%) by weight						
C	**Mn**	**Si**	**P**	**S**	**Ni**	**Mo**	**Al**	**Cr**	**V**	**Cu**
0,084	1,61	0,23	0,01	0,011	0,17	0,17	0,035	0,135	0,015	0,029

Table 2: Parameters of welding [10], [11]

Condition	**(%)**	**V(m/s)**	**I (A)**	**U (V)**
GTAW - R	65	0,0012	152,4	12,04
SMAW - R	80	0,0010	54,2	35,76
SMAW - FP1	80	0,0015	68,8	33,40
SMAW - FP2	80	0,0015	81,8	33,17

pass was done using the same procedure, however, displacement parallel to the XY plane 0.0085m as shown in Fig. (2). In this way, a 3D analysis was employed dividing the plate into 4200 elements of type DC3D8 using a gradient of mesh refinement in size of the elements in X direction, so the region where the heat source passes were concentrates the largest number of elements, as in Fig (2). It was done because the phenomena of thermal transformations have a larger share of calculations performed by the program at this location. The application for the half plate was considered following the theory of symmetry, which allowed obtaining shorter duration of simulation and lower computational cost [12].

One of the key problems for the numerical modeling of a welding process is the modelling material [2]. The majority of the publications on the numerical simulation of welding processes consider that the material properties are highly dependent on temperature. However, it is very difficult to obtain complete information of the dependence on the material properties with temperature, especially to very high temperatures. Simplifications to overcome this problem are often introduced in the numerical simulation of welding processes. Considering that have no information about the physical properties of API 5L X80 steel at different temperature, data of low carbon steel [13], was used as presented in Fig. 3 [4].The values used for density and latent heat for solidification of the weld pool were 7870 kg/m^3 and 270 J/g. The liquid and solid transformation temperature (TL) and (TS) were assumed to be 1480°C and 1430°C respectively [14].

The heat losses by convection were considered for all surfaces of the plate except for the bottom, because the plate was fixed in the table. This condition was adopted to avoid it contact with the environment. The values used for the heat loss by convection (q_c) and radiation (q_r) were 0,77 e 5,6697.10^{-8} W m^{-2} K^4, respectively. It was based on Newton's law of cooling and radiation law, shown in Eq. (3) and Eq. (4), respectively, considering the emissivity and the Stefan Boltzmann constant, to represent the desired welding conditions, the geometry of the heat source was considered and developed in a subroutine DFLUX in Fortran environment. From this it is possible to get different welding conditions by varying parameters such as current, voltage, speed, initial temperature of the plate and interpass temperature. The dimensional parameters of the weld bead is shown in Tab. (3), following the variables shown in Fig. (1). These parameters were measured as described in experimental thermal modeling through a cross section of the welded plate.

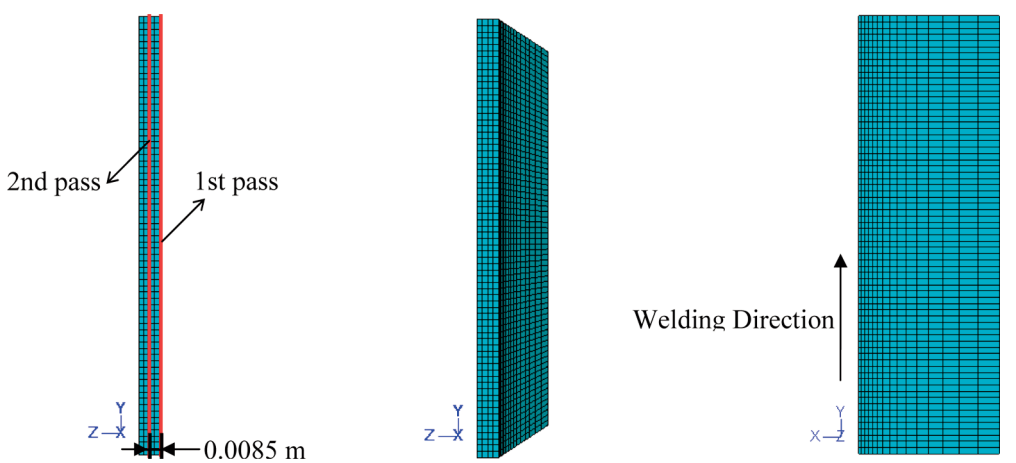

Figure 2: Layout welding and mesh employed in simulation

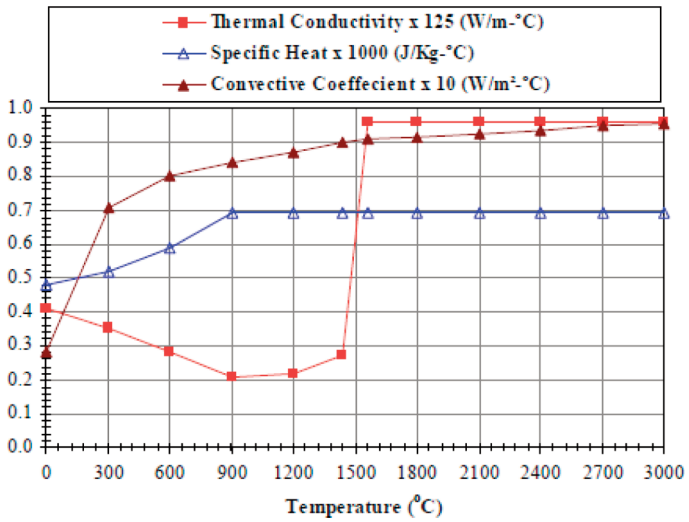

Figura 3: Thermo-physical properties of low carbon steel (AH36) [4]

Table 3: Dimensional parameters of the weld bead

Dimensional Parameters Weld	a_f *(m)*	a_r *(m)*	*b (m)*	*c (m)*
GTAW-R	0,0024	0,0098	0,0024	0,0040
SMAW-R	0,0026	0,0105	0,0026	0,0064
SMAW-FP1	0,0043	0,0172	0,0043	0,0038
SMAW-FP2	0,0045	0,0181	0,0045	0,0031

4. RESULTS AND DISCUSSION

Figure 4 to 6 show the temperature gradient simulation results of multipass welding, for the three conditions, evaluated at time in which the heat source is located in the middle of the plate, at a point such as a thermocouple was coupled in the region simulating a realistic situation, this being the restriction analysis.

Figures 4 and 5 illustrate the thermal gradient of the first and second welding pass, both at the moment when the heat source passes at the center of the plate using the GTAW process for the root pass, and the SWAM process for the hot pass without preheating temperature and preheating of 100°C simultaneously. It can be seen that for these conditions, the peak temperature of the second pass decreased in both cases, however, had wider isotherms as compared to the first pass. This is due to the fact of having increased the welding speed, thus contributing to lower heat input, because the higher the speed, the lower the heat input into the workpiece [11]. In addition, the gradient isotherms for the second pass was larger, due to the energy accumulation from the first pass and the preheating temperature.

Figure 6 shows the thermal gradient of the first and second pass welding, both at the moment when the heat source pass on the center of the plate, using the SMAW process for the root pass and the SWAM process for the hot pass with preheating temperature of 100°C. It can be seen the opposite situation showed in Figures 4 and 5 where the peak temperature

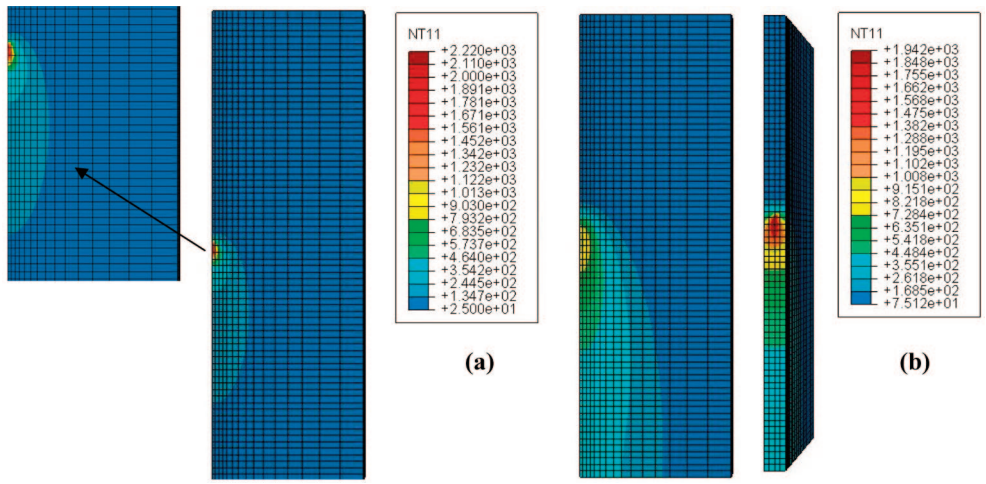

Figure 4: Temperature Gradient: (a) 1st pass (GTAW-R); (b) 2nd pass (SMAW-FP1). (T_0 = 25 °C)

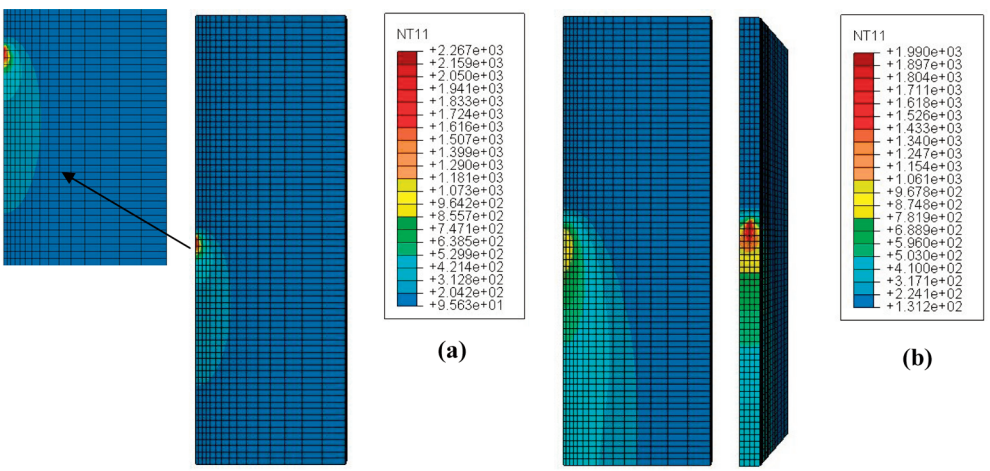

Figure 5: Temperature Gradient: (a) 1st pass (GTAW-R); (b) 2nd pass (SMAW-FP1). (T_0 = 100 °C)

of the second pass, despite the welding speed being the same for the second pass, had a much higher temperature gradient in the first pass, as well as the previous conditions. This happened because it has changed the heat input that was higher by increasing the current value, a fact described by [11], where increasing current values imply an increase in the weld pool.

The thermal cycles of the welded joint on fusion line, using the GTAW-R and SMAW-FP1 welding process with and without preheating and, Fig (7) and using the GTAW-R/SMAW-FP1 and SMAW-R/SMAW-FP2 process Fig. (8) show the comparative thermal cycle between two welding processes, both in the presence of preheating on the same time at which the heat source is passing by the center of the plate.

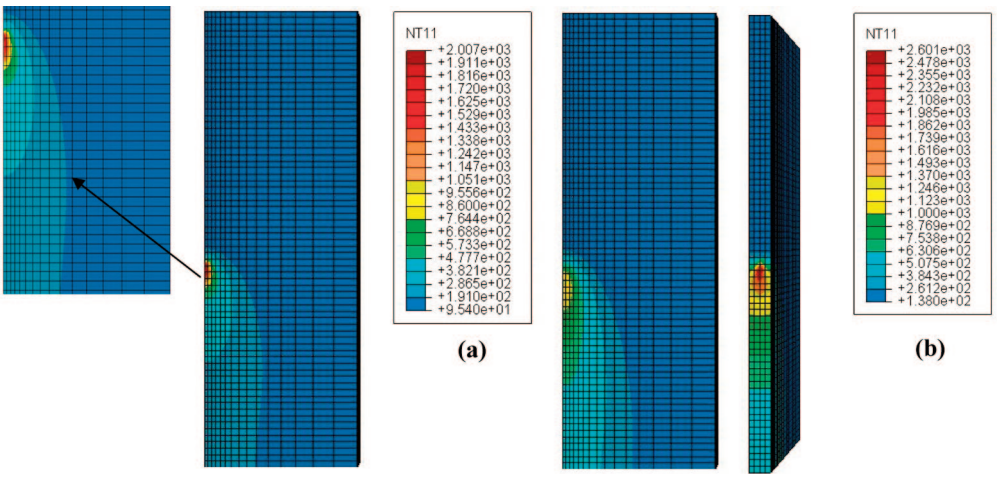

Figure 6: Temperature Gradient: (a) 1st pass (SMAW-R); (b) 2nd pass SMAW-FP2. (T_0 = 100 °C)

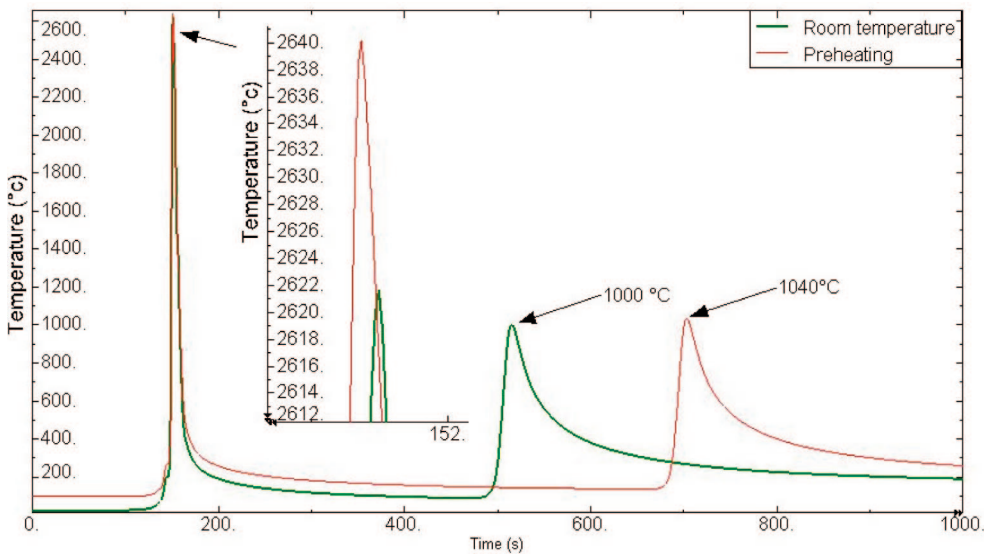

Figure 7: Welding thermal cycle of GTAW-R and SMAW-FP1, varying to the initial temperature

It can be seen as expected, that the first welding pass temperature reached highest peaks in relation to the second pass, because the simulation was done considering a fixed point at the fusion line. In relation to the preheat effect, although it had promoted a little increase in the peak temperature it also promoted a reduction in the cooling rate decreasing the possibility of formation of martensite contributing to the decrease in hardness in the HAZ (Heat Affected Zone), according to the literature [7, 15, 16]. Faster cooling rate can promote the formation of brittle microstructure in HAZ and more large its extension.

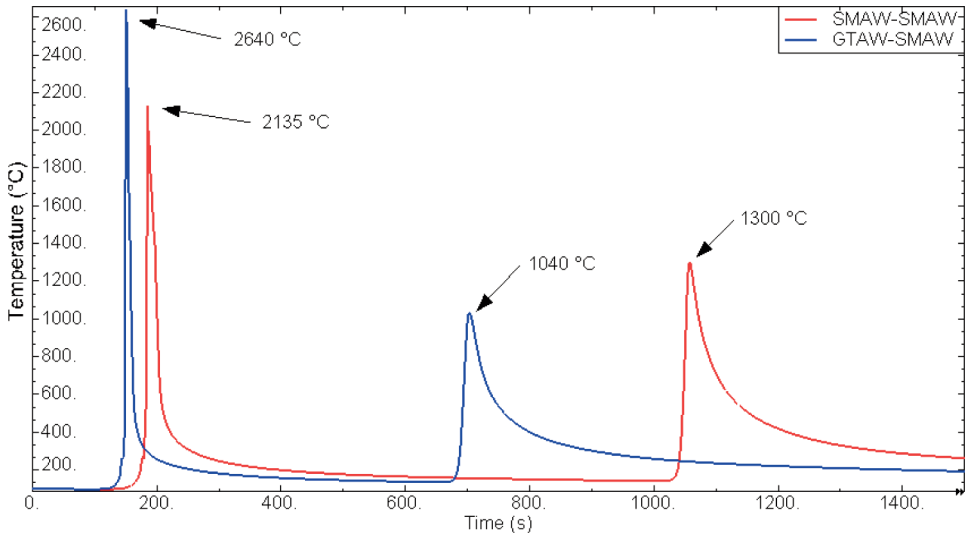

Figure 8: Welding thermal cycle of the process GTAW and SMAW using preheating

By the Figure 8, it can be observed that the weld thermal cycle obtained by GTAW-R and SMAW-FP1 welding process reached higher peak value due to the current value is far higher than those used in SMAW-R and SMAW-FP2 process, however it reached the interpass temperature in a shorter period of time, because the GTAW process has the characteristic to achieve greater heat exchange with the environment and lower efficiency [17].

Weld thermal cycle obtained by [18] of single deposits in HSLA steels with GMAW (Gas Metal Arc Welding), welding process with and without preheating at 100°C is shown in Fig. (9). It was observed, that the application of preheat promoted a longer cooling time with lower cooling rates as it was obtained in this work. Fig. (10) presents weld thermal cycle obtained by Ordonez, of multipass welding in HSLA steel using FCAW process with preheating and interpass temperature of 160°C It can be observed that the author obtained

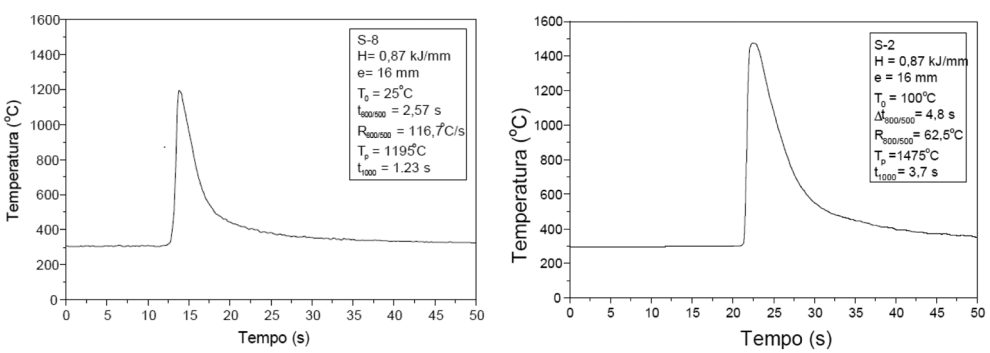

(1) **(2)**

Figure 9: Thermal cycle made experimentally without and with preheating of 100 °C [18]

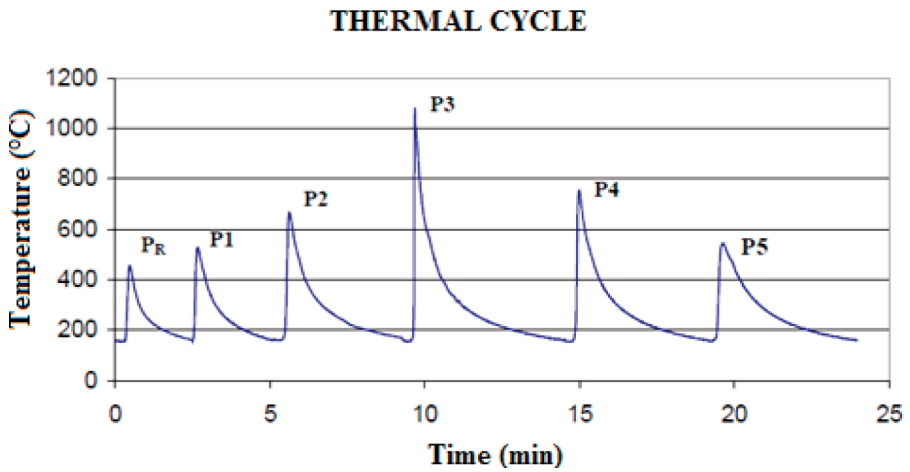

Figure 10: Cycle heat generated by preheating temperature to 160 °C. Adapted from [7]

six weld thermal cycle with thermocouple fixed at one point. It can be observed the reduction of the peak temperature for longer distance from the fusion line, showing a qualitative similarity with the results obtained in the simulation used in this work. This shows the robustness of the computational model.

5. CONCLUSIONS

With the simulation program using the Goldak theory via 3D finite elements, it was possible to evaluate the influence of the welding processes (GTAW and SMAW), demonstrating that the results obtained in the simulation were quite satisfactory, allowing verification the thermal effects provided by the change in the main welding parameters (voltage, current and speed) on the peak temperatures, that is related directly to the cooling curves, whereas for larger values the current, the greater the peak temperature, and for higher speeds, the smaller the energy input to the system, reducing the peak temperature, as also described in [11], showing the robustness of the computer modeling used.

Concerning the study of the effect of preheating, it was possible to evaluate its influence on the thermal welding cycle with a slight increase of the peak temperature, an increase of 2620°C to 2640°C, but of great importance with respect to the cooling curves smoothing, decreasing the rate of cooling could prevent the formation of a brittle HAZ.

The simulation allowed to evaluate similarity to existing experimental results in studies related to welding processes [7, 18], showing the temperature distribution of the workpiece, and the cooling curves at the point of highest temperature, on the fusion line, and the influence of welded region with and without preheating could be serve as reference for future works.

ACKNOWLEDGEMENTS

The authors acknowledge the Academic Unit of Mechanical Engineering and Postgraduate Program in Mechanical Engineering from the Federal University of Campina Grande, CAPES-REUNI for financial support and all entities that finance these research centers.

REFERENCES

[1] Monteiro, L. S., 2004, *Estudo de Ciclos Térmicos de Juntas Soldadas em um Aço de Alta Resistência e Baixa Liga Através do metodo* " In situ" Dissertação de Mestrado em Engenharia Mecânica, Universidade Federal de Campinas. Campinas, SP.

[2] Almeida, D. F. F., 2012. *Determinação das Tensões Residuais e Deformações Resultantes do Processo de Soldadura TIG Através do Método dos Elementos Finitos*, Dissertação de mestrado em Engenharia Mecânica – Faculdade de Ciências e Tecnologia, Universidade de Lisboa, Lisboa.

[3] Bezerra, A. C., 2004. *Análise Térmica do Processo de Soldagem TIG via Elementos Finitos, in Simpósio do Programa de Pós Graduação em Engenharia Mecânica* – Faculdade de Engenharia Mecânica, Universidade Federal de Uberlândia, Uberlândia-MG.

[4] Queresh, E, M.; *Analysis of Residual Stresses and Distortions in Circumferentially Welded Thin-Walled Cylinders*. Thesis (Doctorate in Machanical Engineering) – National University of sciences and Technology, Rawalpindi, Pakistan, 2008.

[5] GUIMARÃES, P. B. Et al.; *Obtaining Temperature Fields as a Function of Efficiency in TIG Welding by Numerical Modeling*. *Thermal Engineering*, v. 10, p. 50–54, 2011.

[6] American Petroleum Institute. API 5 L: *Specification for Line Pipe*. Washington, 42nd ed. January 2000, 153 p.

[7] Cooper Ordóñez, R. E; *Soldagem e Caracterização das Propriedades Mecânicas de Dutos de Aço API 5L-X80 com Diferentes Arames Tubulares*. Dissertação de Mestrado - Campinas, Faculdade de Engenharia Mecânica, Universidade Estadual de Campinas, 2004.

[8] Cooper Ordóñez, R.E.; Silva, J. H. F.; Trevisan, R.E. . *Estudo do comportamento da micro e macrodureza de juntas de aço API X80 soldadas com arame tubular*. In: III Congresso Nacional de Engenharia Mecânica – CONEM, 2004, Belém, PA. III Congresso Nacional de Engenharia Mecânica – CONEM, 2004, 2004.

[9] N-133J – Soldagem, revisão setembro 2002, pp 28–29.

[10] Araújo, B. A, et al.; *Evaluation of the diffusivity and susceptibility to hydrogen ambrittlement of API 5L X80 stell welded joints*. Int. Jnl. Of Multiphysics, Vol. 7(3), 2013, 182–195.

[11] KOU, S. *Welding metallurgy*, 2nd Ed., John Wiley & Sons, 2003.

[12] Jiang, W. G.; *The Development and Applications of the Helically Symmetric Boundary Conditions in Finite Elements Analysis*, *Communications in Numerical Methods in Engineering*. V. 15, p.435–443, (1999).

[13] Nóbrega J. A.; et al.; *Simulação Numérica do Campo de Temperaturas de Juntas Soldadas do aço API 5L X80, Através do Método de Elementos Finitos*, In: XXXIV Iberian Latin-American Congress on Computational Methods in Engineering, Pirenópolis - GO , Brasil, 2013.

[14] Deng, D.; *FEM prediction of welding residual stress and distortion in carbon steel considering phase transformation effects*, Materials and Design, v. p 359–366, 2009.

[15] Srivastava, B.K; Tewari, S. P.; Prakash, J.; *A review on effect of preheating and/or post weld heat treatment (PWHT) on mechanical behavior of ferrous metals* – International Journal of Engineering Science and Technology, v. 2, p 625–631, 2010.

[16] Hinton R.W.; Wiswesser R.W; *Estimating Welding Preheat Requerements for Uknown Grades of Carbon and Low-Allow Steels*, Supplement to the Welding Journal, V. p.78, 2008, 273–278.

[17] Miller, *Guidelines for Gas Tungsten Arc Welding (GTAW)*. available in: http://www.millerwelds.com/pdf/gtawbook.pdf (Accessed on January 26, 2014).

[18] Sobrinho, R. J. F., Alcântara, N. G., 2007. *Análise dos Ciclos Térmicos Obtidos na Zona Afetada Termicamente da Junta Soldada de um Aço de Alta Resistência* in Congresso de Pesquisa e Inovação da Rede Norte Nordeste de Educação Tecnológica" João Pessoa – PB.